ULTRAVIOLET LIGHT EMITTING DIODES EMPLOYING NANOSCALE COMPOSITIONAL INHOMOGENEITIES: A NEW APPROACH FOR TRANSFORMING ARMY ULTRAVIOLET APPLICATIONS

A.V. Sampath, G. A. Garrett, M.L. Reed, E.D Readinger, M. Wraback
U.S. Army Research Laboratory, 2800 Powder Mill Road, Adelphi, MD 20783

C. Chua, N. M. Johnson
Palo Alto Research Center, Palo Alto, CA 94304

ABSTRACT

Nitride semiconductor ultraviolet optical sources offer the possibility of compact, light-weight, low-cost, low-power-consumption optoelectronic sensors that would enable a new generation of fieldable systems for applications that include biodetection, non-line-of-sight covert communications, and water purification. To realize this promise, significant improvements are required in the wall plug efficiency and lifetimes of these devices that are currently limited by the presence of defects in these materials. In this paper we present optical studies of a new material, AlGaN containing nanoscale compositional inhomogeneities, that indicate that active regions containing this material can significantly improve the efficiency of III-Nitride ultraviolet sources. Further, we demonstrate the operation of these active regions within double heterostructure ultraviolet light emitting diodes that further corroborates this conclusion.

1. INTRODUCTION

While many Army applications employing ultraviolet (UV) optoelectronics have been identified, including biodetection, non-line-of-sight covert communications, and water purification, logistical difficulties associated with the size, weight, cost, ruggedness, and reliability of the components has hindered system deployment. III-Nitride semiconductor ultraviolet optical sources offer the possibility of compact, light-weight, low-cost, low-power-consumption optoelectronic sensors that will (1) contribute to the sustainability of the objective force by helping in the reduction of the logistics footprint, and (2) increase tactical options for battlefield commanders, such as stand-off biodetection using a disposable point sensor network. In addition, biodetection, covert communication and water purification based on these devices will provide protection, information, and potable water at the individual soldier level, aiding the survivability, lethality, and deployability of the current and future force.

Typical III-Nitride semiconductor-based UV light emitting diodes (UV LEDs) employing multiple-quantum-well (MQW) active regions have wall plug efficiencies and lifetimes far less than those of commercially available blue LEDs (Zhang *et al.*, 2005). These limitations are due to a large density of defects caused by heteroepitaxial growth of these III-Nitride based devices on lattice mismatched substrates that reduce their efficiency and increase debilitating heating. Recently, we have reported on the development of AlGaN films deposited by plasma assisted molecular beam epitaxy (PA-MBE) that possess enhanced internal quantum efficiency due to the presence of nanometer scale compositional inhomogeneities (NCI-AlGaN) within a wider band gap matrix that inhibit nonradiative recombination through the large defect densities in these materials (Collins *et al.*, 2005). These NCI-AlGaN films exhibit intense room temperature photoluminescence (PL) that is ~ 1000x stronger than, and greater than 250 meV red-shifted with respect to, the normally expected band edge emission.

In this paper, we report on the unique nanoscale aspects of this new material that lead to concomitant suppression of nonradiative recombination and reduction of radiative lifetime for improved radiative efficiency. We also discuss the performance of double heterostructure (DH) UVLEDs employing a NCI-AlGaN active region that demonstrates the potential of these nanoscale compositional inhomogeneities to improve the quantum efficiency and overall performance of UV light emitters.

2. EXPERIMENTAL

All of the films investigated were deposited by plasma assisted molecular beam epitaxy (PA-MBE) using a Varian GeNII Molecular Beam Epitaxy reactor. These samples consisted of AlGaN epilayers containing ~ 40% AlN by mole fraction deposited upon c-plane sapphire substrates using a three-step deposition method that has been reported previously (Sampath *et al.*, 2006).

Time-resolved data is obtained using two techniques: (1) gated downconversion, with temporal resolution of ~ 300 fs, time scale of ~ 1 ns, and a dynamic range enabling ~ 2 orders of magnitude variation in photoexcited carrier density; and (2) time-correlated single photon counting,

Report Documentation Page

Form Approved
OMB No. 0704-0188

1. REPORT DATE	2. REPORT TYPE	3. DATES COVERED
01 NOV 2006	**N/A**	**-**

4. TITLE AND SUBTITLE	5a. CONTRACT NUMBER
Ultraviolet Light Emitting Diodes Employing Nanoscale Compositional Inhomogeneities: A New Approach For Transforming Army Ultraviolet Applications	5b. GRANT NUMBER
	5c. PROGRAM ELEMENT NUMBER
6. AUTHOR(S)	5d. PROJECT NUMBER
	5e. TASK NUMBER
	5f. WORK UNIT NUMBER
7. PERFORMING ORGANIZATION NAME(S) AND ADDRESS(ES) **U.S. Army Research Laboratory, 2800 Powder Mill Road, Adelphi, MD 20783**	8. PERFORMING ORGANIZATION REPORT NUMBER
9. SPONSORING/MONITORING AGENCY NAME(S) AND ADDRESS(ES)	10. SPONSOR/MONITOR'S ACRONYM(S)
	11. SPONSOR/MONITOR'S REPORT NUMBER(S)

12. DISTRIBUTION/AVAILABILITY STATEMENT
Approved for public release, distribution unlimited

13. SUPPLEMENTARY NOTES
See also ADM002075., The original document contains color images.

14. ABSTRACT

15. SUBJECT TERMS

16. SECURITY CLASSIFICATION OF:			17. LIMITATION OF ABSTRACT	18. NUMBER OF PAGES	19a. NAME OF RESPONSIBLE PERSON
a. REPORT	b. ABSTRACT	c. THIS PAGE			
unclassified	**unclassified**	**unclassified**	**UU**	**6**	

with temporal resolution of ~ 25 ps, time scale of up to 4000 ns, and a dynamic range enabling up to 5 orders of magnitude variation in photoexcited carrier density. Complementary time-integrated PL measurements are performed using a cw- 244 nm frequency-doubled argon ion laser. Both time-resolved and time-integrated PL data are taken in the 10K to 300K temperature range using a compressed helium-cooled cryostat.

3. OPTICAL STUDIES OF NANOSCALE COMPOSITIONAL INHOMOGENEITIES IN ALGAN

Previously we have demonstrated that NCI-AlGaN alloys containing as much as 60% AlN by mole fraction can be deposited by controllably varying the Al metal atom flux employed during growth (Sampath *et al.*, 2006). The peak wavelength of the PL spectra for these alloys moves progressively towards shorter wavelength with increasing alloy band gap. To understand the role of the redshift in these active regions a series of 40% NCI-AlGaN films were deposited with varying magnitude of redshift by modifying the conditions of growth. Figure 1 shows that the room temperature (RT) PL under CW-excitation increases with the redshift. However, comparison of two samples in the series shows that sample A, with the larger shift and brighter RT PL, has dimmer PL at low temperature (11K) than sample B. Femtosecond TRPL using gated down-conversion provides a possible explanation of this behavior, since the dynamics of carrier transfer from the band edge matrix to the NCI region can be seen. The fact that sample A has NCI emission twice as bright as sample B under cw-excitation is reflected in the TRPL by a longer RT lifetime in Sample A, ~ 459 ps verses 313 ps (Fig. 2). Sample B also has a faster decay in the band edge matrix PL that suggests a more rapid transfer of carriers to a larger density of NCI states in this film than sample A. This explanation is corroborated by the observation that the peak signal for the NCI emission near time-zero for

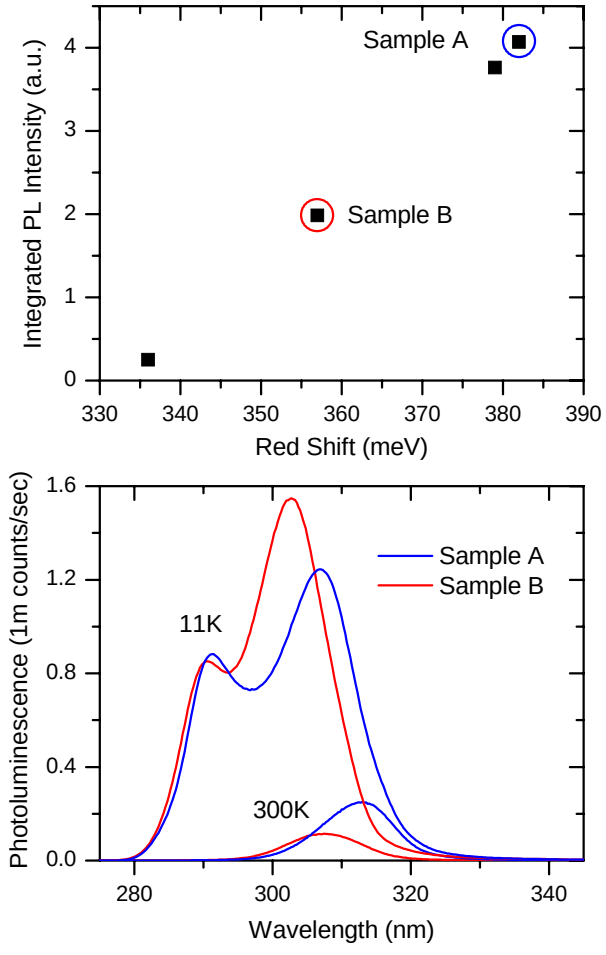

Fig. 1. Room-temperature photoluminescence (PL) intensity dependence on redshift for NCI AlGaN samples (top); Room- and low- temperature PL spectra for two samples in the series (bottom).

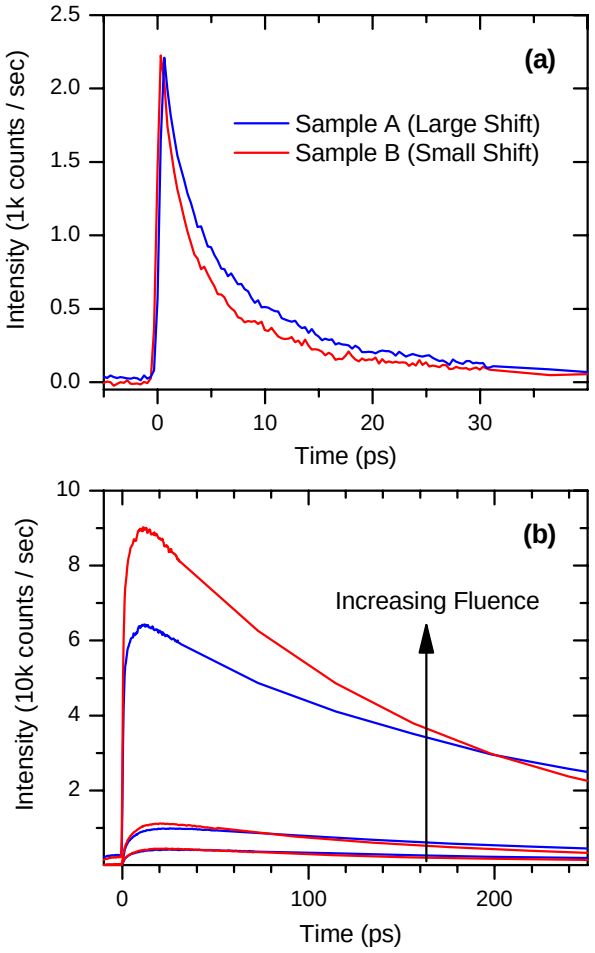

Fig. 2. Band edge luminescence at high pump intensity **(a)** and pump intensity dependent NCI luminescence **(b)** as a function of time delay for the two samples.

sample A becomes smaller than for sample B with increasing pump intensity due to saturation of the smaller density of NCI states in sample A, and is further supported by the larger time integrated PL intensity in sample B at temperatures low enough that nonradiative recombination paths are frozen out. The shorter RT lifetime at densities high enough to saturate nonradiative centers within the NCI for sample B suggests that the individual NCI regions in this sample may be smaller, with a larger relative density of interface states that may mediate nonradiative recombination through unsaturated defect states in the wider band gap matrix. However, while the smaller redshift of the NCI emission peak in moving from 11K to RT in sample B relative to sample A (64 meV vs. 75 meV) supports the notion that the average size of the NCI in sample B may be smaller, with concomitant reduced electron-phonon interaction, the shifts in both samples are too large to invoke quantum confinement (Brown *et al.*, 2001). Rather, the smaller nonradiative lifetime (333 ps vs. 546 ps) and longer radiative lifetime (5.2 ns vs. 2.9 ns) in sample B relative to sample A under low excitation conditions at room temperature imply that one of the main reasons for the shorter PL lifetime and weaker time-integrated PL in this

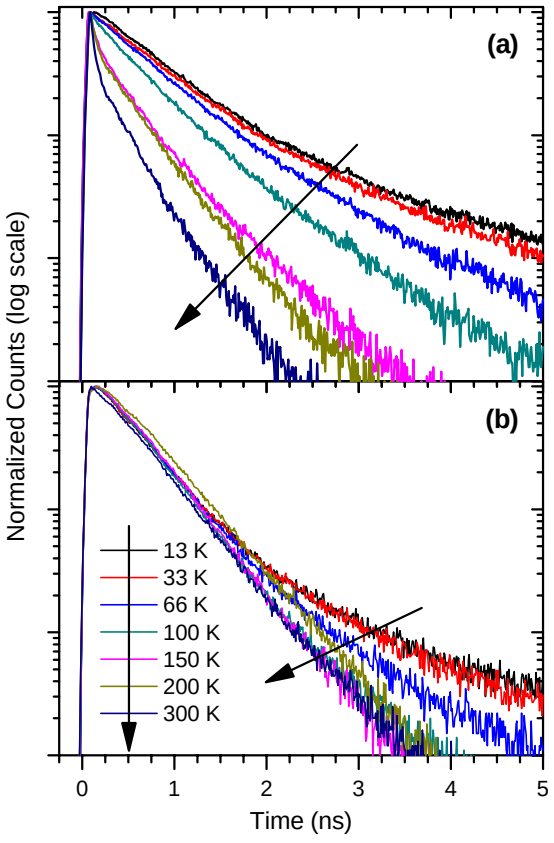

Fig. 3. Time-resolved PL as a function of temperature for **(a)** band edge bulk and **(b)** localized NCI material emission. A pump excitation fluence of 2.8 μJ/cm^2 (est. carrier density of 4×10^{17}cm^{-3}) at 285 nm was used.

sample may be the lower carrier density in the NCI associated with the relatively larger density of NCI regions.

An even smaller red shift of the NCI emission might be associated with a relative blue shift due to quantum confinement. Figure 3 shows TRPL on a sample with a redshift of 300 meV, smaller than that in Sample B, but which is brighter than Sample A, most likely due to a thick, possibly lower defect density, base layer on which it was grown. As temperature is decreased from 300 K to 13 K, PL emission from the band edge arises from the noise to about 20% that of the NCI red-shifted peak, and its lifetime increases from a system response limit of 25 ps to over 600 ps. This behavior is related to the freeze out of nonradiative sites and localization of carriers in the bulk, wider band gap matrix (Cho *et al.*, 2000, Kim et al, 2000). For the NCI peak, an approximately constant lifetime of 450 ps is observed as a function of temperature and an internal quantum efficiency of ~28% is estimated from the ratio of the low- and room-temperature PL intensities. Figure 4 shows the calculated radiative lifetimes for the NCI and band edge emissions. Since it is difficult to determine the intensity of the band edge emission corresponding to the wider band gap matrix at temperatures above 150K, the radiative lifetime for band edge emission is only an estimated lower bound. On the other hand, the radiative lifetime for NCI represents an upper bound due to a continuous transfer of carriers from the matrix to the NCI region. The radiative lifetime for band edge emission is consistent with measured values for GaN and with the theoretical value at equivalently doped GaN (Im *et al.*, 1997, Brandt *et al.*, 1998). The radiative lifetime for the red-shifted emission from the NCI is almost independent of temperature, reaching a value of ~ 2 ns at room temperature. One reason for this may be the large amount of carriers transferred from the matrix to the NCI. Theoretical calculation indicates the temperature

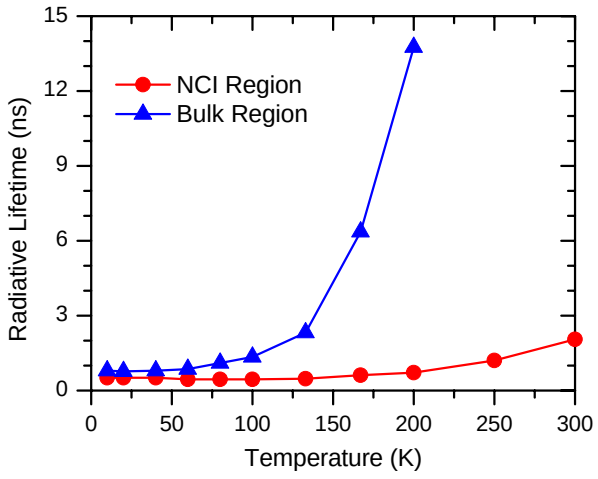

Fig. 4. Radiative lifetimes calculated from PL lifetimes and estimated internal quantum efficiencies.

dependence of the radiative lifetime is significantly reduced when the carrier density is high. (Im *et al.*, 1997). On the other hand, it is well known that the radiative lifetime of a zero dimensional exciton is nearly constant over temperature. This suggests a lower dimensionality of the NCI region. This idea is supported by a smaller measured shift in the NCI PL peak, from room to low temperature, of 48 versus 75 meV for the 300 versus 400 meV red-shift samples due to a reduction of the electron-phonon interaction in the smaller structures.

Further insight can be obtained from the room temperature, intensity dependent TRPL data in Fig. 5 from a double heterostructure (DH) LED structure on an AlGaN template with the NCI AlGaN as the active region. In this case, the pump pulse is tuned to 265 nm to include photogeneration of carriers in the barrier region of the structure. The PL lifetime at low fluence (< 20 $\mu J/cm^2$) increases by nearly a factor of two in the DH LED structure relative to similar layers on sapphire, with a half-life of ~ 500 ps, and a dominant decay time in excess of 700 ps. Although this sample has dislocation density in the mid $10^{10} cm^{-2}$ range, the decay times are comparable to those measured in high quality MBE GaN grown atop HVPE GaN templates with dislocation densities in the mid $10^{7} cm^{-2}$ range (Kwon et al, 2000, Sampath *et al.*, 2004),. suggesting that the further suppression of nonradiative recombination processes within and at the boundaries of the NCI regions also contributes to the increased internal quantum efficiency in the DH LED structure. While the PL decay shows no intensity dependence at low densities, it exhibits a dramatic decrease in the half-life at the highest fluence (128 $\mu J/cm^2$) to 292 ps that is associated with the onset of a fast decay component. This drop in the PL decay time may be indicative of a decrease in the radiative lifetime at high carrier densities due to nonlinear radiative recombination in the localized regions, which may be driven by enhanced carrier concentrations associated with the transfer of carriers from the AlGaN matrix to the smaller localized regions and the suppression of nonradiative processes in these regions. Thus, the combination of saturation of nonradiative recombination sites through carrier transfer from the matrix and concentration in the NCI and concomitant lower radiative lifetimes of the NCI relative to the matrix, associated with the higher concentration in and possibly lower dimensionality of the NCI, provides an attractive option for development of high efficiency UV LEDs.

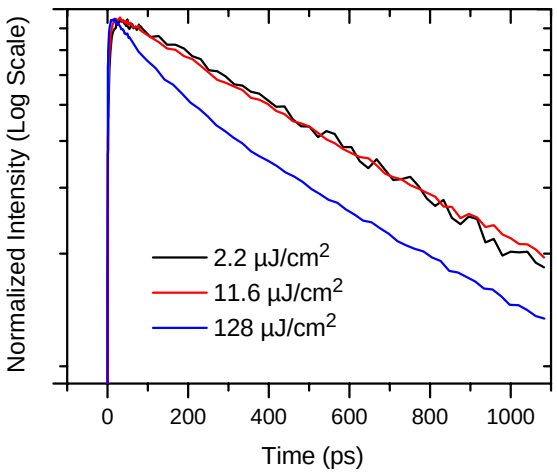

Fig. 5. Intensity dependent room-temperature TRPL from a DH UVLED structure taken at the 330 nm peak corresponding to NCI emission.

4. DOUBLE HETEROSTRUCTURE UVLEDS

The viability of the NCI-AlGaN active region has been further verified by incorporating them into double heterostructure (DH) UVLEDs designed for 320 nm emission. These structures consist of a highly conductive n-type AlGaN base layer ($n=1x10^{19}$ cm^{-3}) containing ~40% AlN by mole fraction so as to be transparent at the emission wavelength and allow for back-side or substrate-side light extraction. Subsequently a Si doped, n-type, 50 nm thick NCI-AlGaN active region was deposited. Next, a 6 nm thick AlGaN electron blocking layer was deposited containing ~40% AlN by mole fraction. This layer was doped with Mg to induce p-type conductivity. Finally a 100 nm thick p-type GaN layer ($p=8x10^{17}$ cm^{-3}) was deposited. Device layers were deposited on n-type AlGaN templates grown by metalorganic chemical vapor deposition (MOCVD). These highly conductive MOCVD AlGaN layers were grown AlGaN templates deposited by hydride vapor phase epitaxy on c-plane sapphire substrates.

Back-emitting light emitting diodes were fabricated by first etching 50x50, 100x100 or 200x200 μm^2 mesas using an inductive coupled plasma reactive ion etcher and a Cl2 chemistry. Subsequently, Ti/Al/Ni/Au n- metal contact layers and Ni/Au p- metal contact layers were deposited by electron beam evaporation and defined by standard photolithograpy lift-off processes.

Figure 6 shows representative L-I characteristics for these unpackaged DH-UVLEDs. An output power of 0.45 mW at a DC drive current of 60 mA was measured for a 100x100 µm device. The output power of these devices rolls over for drive currents in excess of 50 mA to due to deleterious heating that can be minimized by packaging the device die with appropriate heatsinking. The electroluminescence of these devices is characterized by a sharp peak at 325 nm with a FWHM of 12 nm that is comparable to what is seen in MQW UVLEDs (Fig. 7). Moreover, we observe that the out-of-band, low energy, emission is ~2 orders of magnitude lower than the NCI emission at 325 nm, which is important for bioagent

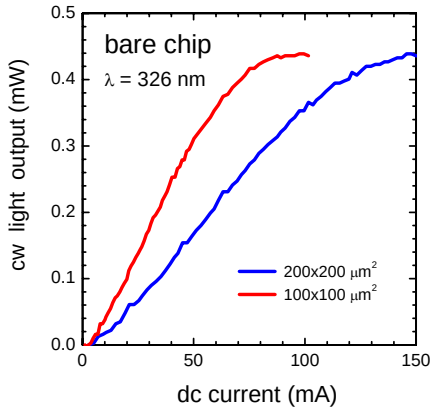

Fig. 6. Light output versus current for double heterostructure UVLEDs with different device sizes.

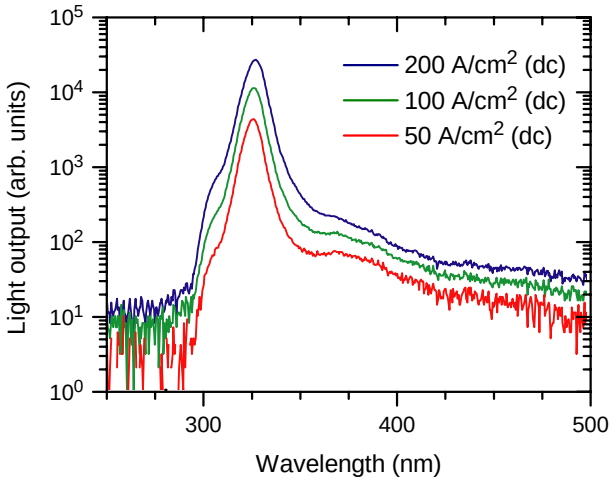

Fig. 7. Electroluminescence spectrum from a double heterostructure UVLED as a function of current density.

detection applications. An external quantum efficiency of 0.26% was determined for a 50x50 μm^2 device die, which is reasonable for an unpackaged device.

Furthermore, while these results are comparable to those typical of conventional MQW UVLEDs, it is important to note that a DH-UVLED of similar active region thickness using conventional layers without the benefit of the NCI would have orders of magnitude less output power than our device due to the strong polarization fields normally found in wurtzite c-plane nitride semiconductor heterostructures. These fields reduce the electron-hole wavefunction overlap, thereby suppressing radiative recombination in these materials while red-shifting the emission peak with respect to band gap. The enhanced PL intensity with increasing redshift in the AlGaN NCI material illustrated in Fig. 1 suggests that polarization fields do not play a significant role in the NCI emission, perhaps due to the large concentration of carriers in the NCI. Together these results provide strong evidence that the deleterious polarization fields present in conventional c-plane nitride semiconductor devices are suppressed in our NCI-AlGaN active regions without the implementation of non-polar growth orientations, pointing the way toward devices with significantly improved external quantum efficiencies.

5. CONCLUSIONS

Temperature and intensity dependent TRPL measurements on a new material, AlGaN containing nanoscale compositional inhomogeneities (NCI), show that it inherently combines inhibition of nonradiative recombination with reduction of radiative lifetime, providing a potentially higher efficiency UV emitter active region. Double heterostructure LEDs employing NCI-AlGaN as an active region have been demonstrated and suggest that deleterious polarization fields present in conventional c-plane nitride semiconductor devices are suppressed in our NCI-AlGaN active regions without the implementation of nonpolar growth orientations, pointing the way toward devices with significantly improved external quantum efficiencies.

ACKNOWLEDGEMENTS

The authors would like to thank V. Dmitriev of TDI, Inc. for the AlGaN template used for the NCI AlGaN DH LED structure and helpful discussions.

REFERENCES

Brandt, O., J. Ringling, K.H. Ploog, H.-J. Wunsche, and F. Henneberger, "Temperature dependence of the radiative lifetime in GaN," *Phys. Rev.*, Vol. B58, No. 24, pp. R15977-R15980, December, 1998.

Brown, J, C. Elsass, C. Poblenz, P.M. Petroff, and J.S. Speck, "Temperature dependent photoluminescence of MBE grown gallium nitride quantum dots," *Phys. Stat. Sol.*, Vol. 228, No. 1, pp.199-202, November 2001.

Cho, Y.-H., G.H. Gainer, J.B. Lam, and J.J. Song, "Dynamics of anomalous optical transitions in $Al_xGa_{1-x}N$ alloys," *Phys. Rev.*, Vol. B61, No. 11, pp.7203-7206, March, 2000.

Collins C.J., A.V. Sampath, G.A. Garrett, W.L. Sarney, H. Shen, M. Wraback, A.Yu. Nikiforov, G.S. Cargill, III, and V. Dierolf, "Enhanced room temperature luminescence efficiency through carrier localization in AlGaN alloys," *Appl. Phys.Lett.*, Vol 86, pp 031916-1-3, January 2005.

Kim, H.S., R.A. Mair, J. Li, J.Y. Lin, and H.X. Jiang, "Time-resolved photoluminescence studies of $Al_xGa_{1-x}N$ alloys," *Appl. Phys. Lett.*, Vol. 76, No. 10, pp. 1252-1254, March, 2000.

Kwon, H.K., C.J. Eiting, D.J.H. Lambert, M.M. Wong, R.D. Dupuis, Z. Liliental-Weber, and M. Benamara,

"Observation of long photoluminescence decay times for high-quality GaN grown by metalorganic chemical vapor deposition," *Appl. Phys. Lett.*, Vol. 77, No. 16, pp. 2503-2505, October, 2000.

Im, J.S., A. Moritz, F. Steuber, V. Harle, F. Scholz, and A. Hangleiter, "Radiative carrier lifetime, momentum matrix element, and hole effective mass in GaN," *Appl. Phys. Lett.*,Vol. 70, No. 5, pp. 631-633, February 1997

Sampath A.V, G.A. Garrett, C.J. Collins, P. Boyd, J. Choe, P.G. Newman, H. Shen, M. Wraback, R.J. Molnar and J. Caissie, "Effect of Ga rich growth conditions on the optical properties of GaN films grown by plasma-assisted molecular beam epitaxy," *J. Vac. Sci. Technol*, Vol. B22, No. 3, pp. 1487-1490, May, 2004.

Sampath A.V., G.A. Garrett, C.J. Collins, W.L. Sarney, E.D. Readinger, P.G.Newman, H. Shen, M. Wraback," Growth of AlGaN Alloys Exhibiting Enhanced Luminescence Efficiency," *J. Electron. Mat.*, Vol 35, No 4, pp. 641-646, April 2006

Zhang J., X. Hu, A. Lunev, J. Deng, T.M. Katona, M.S. Shur, R. Gaska, M. A. Khan, "AlGaN Deep Ultraviolet Light Emitting Diodes," *Japan. J. Appl. Phys Part 1.*,Vol 44, No. 10 . pp. 7250-7253, October 2005